



Cite this: DOI: 10.1039/d0nj03226c

Catalytic performance of benzoxazine derived ordered mesoporous carbon materials for the selective oxidation of 2-methylnaphthalene

 Zhouxuan Zang, Yingge Chang, Yi Yu, Haihan Zhang, Li Xu * and Guoji Liu 

2-Methylnaphthoquinone is an important chemical product. The catalyst used in the catalytic oxidation of 2-methylnaphthalene to 2-methylnaphthoquinone has been a research hotspot. In this paper, benzoxazine derived ordered mesoporous carbon materials were used as catalysts, and their catalytic performance in acetic acid/hydrogen peroxides was investigated. The N/S co-doped carbon material (NSCM) was prepared with thiourea-type benzoxazine as a carbon precursor and SBA-15 as a template. The nitrogen-doped carbon material (NCM) was prepared using the same method using aniline-type benzoxazine as a precursor. The carbon materials were characterized by N₂ adsorption/desorption, X-ray diffraction (XRD), scanning electron microscopy (SEM), transmission electron microscopy (TEM), X-ray photoelectron spectroscopy (XPS) and Raman spectroscopy. The results have shown that both carbon materials exhibit worm-like structure and have graphitized amorphous structure. Nitrogen in the carbon materials existed in the form of pyridine nitrogen and pyrrole nitrogen, which caused the surface defects of carbon materials. The surface defects are critical for the enhancement of the catalytic activity of carbon materials. With NSCM and NCM as catalysts, the yields of 2-methylnaphthoquinone were 78.8% and 65.7%, respectively. By comparison, NSCM has higher catalytic activity, and the catalytic activity remains stable after five cycles of use. These results indicate that NSCM has great potential as a highly efficient catalyst for the selective oxidation of 2-methylnaphthalene.

 Received 2nd July 2020,
 Accepted 16th September 2020

DOI: 10.1039/d0nj03226c

rsc.li/njc

1. Introduction

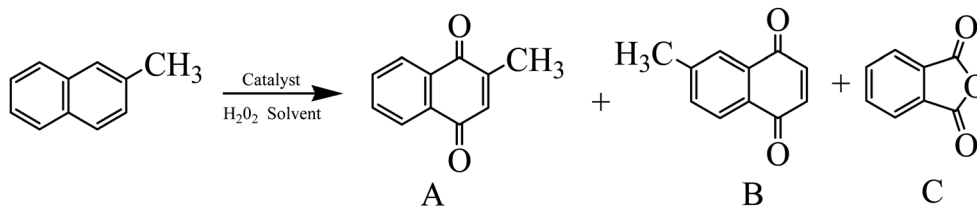
2-Methylnaphthoquinone is an important intermediate for K-type vitamins, and it is also known as 2-methyl-1,4-naphthoquinone or β -methyl-1,4-naphthoquinone.^{1,2} The schematic diagram of the products of 2-methylnaphthalene oxidation is given in Scheme 1. Compound A is 2-methyl-1,4-naphthoquinone which is the major product and B and C are 6-methyl-1,4-naphthoquinone and phthalic anhydride, respectively, which are the supernumerary products.

In industry, sulfuric acid/chromic anhydride (or sodium dichromate) is used to oxidize 2-methylnaphthalene to synthesize 2-methyl-1,4-naphthoquinone, but this method produces a lot of waste water containing chromium, which causes serious environmental pollution.³ So, in recent years, a large number of studies have been carried out on non-chromium heterogeneous catalytic systems. And various catalysts have been developed for the liquid–solid phase method, for example, molecular sieves, ionic liquids, and metal oxides. Zi⁴ had studied the catalytic performance of lanthanum doped MCM-41 as a catalyst for the preparation of 2-methyl-1,4-naphthoquinone by the liquid–solid

phase oxidation of 2-methylnaphthalene. The MCM-41 catalyst exhibited excellent catalytic performance under mild conditions, and the yield of 2-methyl-1,4-naphthoquinone can reach 65.6%. Serhan Uruş⁵ had used silica-supported metal ions (Ru²⁺, Pd²⁺, Co²⁺) as catalysts for the catalytic oxidation reaction of 2-methylnaphthalene. Oxana A. Kholdeeva⁶ had used silica supported iron phthalocyanine as a catalyst to catalyze the oxidation of 2-methylnaphthalene. However, the metal-based catalysts also have significant disadvantages, including high cost, poorer durability, lower selectivity, prone to poisoning, and environmental pollution.⁷ Therefore, it is of great practical significance to search for a mild, clean and efficient 2-methylnaphthalene liquid–solid phase oxidation catalyst.

Due to the unique physical and chemical properties of carbon materials, their application in the field of catalysis has attracted the attention of many scholars in recent years. An increasing number of carbon materials had been developed and applied as catalysts.⁸ Hiroyuki Watanabe⁹ had used activated carbon as a raw material to prepare nitrogen-doped carbon materials and tested their catalytic performance through the catalytic oxidation of several alcohols. The results showed that nitrogen-doped activated carbon was catalytically active in partial alcohol oxidation. Eldar Zeynalov¹⁰ had used

School of Chemical Engineering, Zhengzhou University, Zhengzhou, China



Scheme 1 Schematic diagram of catalytic oxidation of 2-methylnaphthalene.

CNTs as catalysts to catalyze the oxidation of hydrocarbons and explored the effects of carbon nanotube impurities. Song¹¹ had suggested that the surface defects of carbon materials may be active sites. H₂O₂ molecules can be adsorbed on the defect sites on the surface of carbon tubes and decompose into active oxygen molecules. The presence of heteroatoms can cause surface defects in carbon materials, which determines them to be multifunctional carbon-based metal-free catalysts. Doping of heteroatoms is an effective way to enhance the catalytic performance of carbon materials.^{12–14} Su¹⁵ had notably improved the catalytic activity of carbon materials through doped heteroatoms. And a large number of reports have indicated that heteroatom-doped carbon materials can exhibit excellent catalytic performance in many liquid-phase reactions.^{16–21}

So far, most of the carbon-based metal-free catalysts are used in the field of clean and sustainable energy, but few studies have applied them in the chemical synthesis area. In view of the *status quo* of the oxidation of 2-methylnaphthalene to a 2-methyl-1,4-naphthoquinone catalytic system described above, in combination with the good performance of carbon materials in different oxidation reactions, we attempted to apply cheap and readily available carbon materials to the oxidation of 2-methylnaphthalene to form a 2-methyl-1,4-naphthoquinone catalytic system, to explore the application of carbon material catalysts in traditional chemical synthesis.

Polybenzoxazines (PBZs), a new type of heterocyclic polymers, are known as promising carbon precursors for high-performance nitrogen doped carbon materials, because of their nitrogen content, molecular design flexibility, high char yield and excellent thermal stability. Due to the good molecular design flexibility, the incorporation of heteroatoms into the carbon framework can be achieved by selecting phenols or primary amines containing heteroatoms to synthesize benzoxazine monomers.²²

In this study, the different types of benzoxazine (BOZ) were used as the precursor, and the nitrogen-doped and N/S co-doped carbon materials were prepared using the hard template method. Two carbon materials were used as catalysts in the oxidation of 2-methylnaphthalene and the main influencing factors were investigated.

2. Experimental

2.1. Materials

Thiourea, aniline, phenol, formaldehyde solution (mass score 37%), toluene, acetic acid, and tetrahydrofuran were all analytical

reagents purchased from Comeo reagents. SBA-15 is purchased from Xfnano company, and H₂O₂ (mass score 30%) is purchased from Luoyang Reagent Factory. The chemicals were used as received without any further purification.

2.2. Preparation of carbon materials

2.2.1. Synthesis of the thiourea-type benzoxazine. The benzoxazine is synthesized using the solvent method as follows: thiourea and toluene were added together to the three-necked flask and the three-necked flask was stirred in an oil bath, while formaldehyde was added. After stirring for 1 h, the phenol dissolved in toluene was added. After half an hour, the temperature of the oil bath was raised to 115 °C, and the condensation was refluxed for 6 h. When the reaction was completed, the washing with 1 mol L⁻¹ NaOH solution and suction filtration were performed. Finally, the filtrate was distilled off. The product was poured into a beaker and dried under vacuum at 65 °C for 24 h. The formula of the thiourea-type benzoxazine is shown in Fig. 1.

2.2.2. Synthesis of the aniline-type benzoxazine. The synthesis of the aniline-type benzoxazine is the same as 2.2.1, except that thiourea has been replaced by aniline. The formula of the aniline-type benzoxazine is shown in Fig. 2.

2.2.3. Preparation of carbon materials. In this experiment, both carbon materials were prepared using a hard template method. Certain amount of the benzoxazine monomer was placed in a vial and dissolved with an appropriate amount of tetrahydrofuran. And an equal amount of SBA-15 was added and immersed for about 5 h. Throughout the immersing process, the temperature was controlled at 30–35 °C. Then, the obtained solid mixture was cured at 120 °C, 140 °C, 160 °C, 180 °C, 200 °C and 220 °C for 2 h, respectively. The cured mixture was carbonized under the N₂ atmosphere at 400 °C and 800 °C for 2 h, respectively with the heating rate 2 °C min⁻¹. After carbonization, 50% HF was used to etch away the template agent and washed with deionized water until it becomes neutral. The carbon materials were dried at 80 °C. Carbon materials with thiourea-type benzoxazine and aniline-type benzoxazine as precursors are, respectively, named the N/S

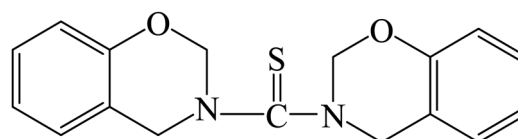


Fig. 1 Formula of the thiourea-type benzoxazine.

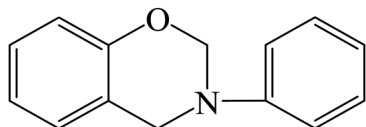


Fig. 2 Formula of the aniline-type benzoxazine.

co-doped carbon material (NSCM) and nitrogen-doped carbon material (NCM) in this paper.

2.3. Characterization of materials

The two types of benzoxazines were characterized by FTIR (FT-IR200, America). The carbon materials were characterized using the N_2 adsorption/desorption test (Autosorb-iQ, America), XRD (D8 Advance, Germany), SEM (JSM-7500F, Japan), TEM (TalosF200S, America), and XPS techniques (AXIS Supra, Japan).

2.4. Experiment for 2-methylnaphthalene catalytic oxidation

In this experiment, acetic acid was used as a reaction solvent and hydrogen peroxide as an oxidant. The reaction was carried out in a 50 mL three-necked flask by adding a certain amount of raw materials and carbon material catalysts, and simultaneously adding acetic acid. H_2O_2 was added dropwise after the reaction mixture was heated to the set temperature. After the reaction, the temperature was naturally lowered and the catalyst was filtered under reduced pressure. The products were analyzed by Agilent 7890B gas chromatography, and the yield of 2-metaphthoquinone is used as the evaluation index of catalyst performance. The $n_0(C_{11}H_{10})$ and $n(C_{11}H_{10})$ are the amounts of 2-methylnaphthalene before and after the reaction. The amount of 2-menadione is represented by $n(C_{11}H_8O_2)$. The conversion of 2-methylnaphthalene and the selectivity of 2-methylnaphthoquinone were calculated as follows:

$$X_{C_{11}H_{10}} (\%) = \frac{n_0(C_{11}H_{10}) - n(C_{11}H_{10})}{n_0(C_{11}H_{10})} \times 100\%$$

$$S_{C_{11}H_8O_2} (\%) = \frac{n(C_{11}H_8O_2)}{n_0(C_{11}H_{10}) - n(C_{11}H_{10})} \times 100\%$$

3. Results and discussion

3.1. FTIR spectra of benzoxazines

Fig. 3(a) shows the FTIR spectra of thiourea-type benzoxazine. It can be seen from Fig. 3(a) that 757 cm^{-1} is the out-of-plane bending vibration absorption peak of the benzene ring C–H, and 933 cm^{-1} is the characteristic absorption peak of the oxazine ring. The peaks at 1234 cm^{-1} and 1365 cm^{-1} are the stretching vibration absorption peaks of the C–O–C and C–N–C bonds on the oxazine ring, respectively. 1595 cm^{-1} is the characteristic absorption peak of the benzene ring skeleton. Fig. 3(b) shows the FTIR spectra of aniline-type benzoxazine. The out-of-plane bending vibration absorption peak of benzene ring C–H is 754 cm^{-1} . 945 cm^{-1} is the characteristic absorption peak of the oxazine ring. The peaks at 1156 cm^{-1} and 1227 cm^{-1} are the symmetric and asymmetric stretching vibration absorption peaks of C–O–C on the oxazine ring, respectively. 1371 cm^{-1} is the C–N–C stretching vibration absorption peak on the oxazine ring. 1496 cm^{-1} and 1597 cm^{-1} are the characteristic absorption peaks of the benzene ring skeleton. The characterization results have confirmed the successful synthesis of two types of benzoxazines.

3.2. N_2 adsorption/desorption of carbon materials

Fig. 4 shows the N_2 adsorption/desorption isotherm and BJH pore size distribution plots of two carbon materials. The adsorption/desorption isotherms of both carbon materials are typical IV adsorption/desorption isotherms, which indicates the mesoporous structure of carbon materials.²³ For the nitrogen-doped carbon material, the specific surface area is $674.04\text{ m}^2\text{ g}^{-1}$, pore volume is $1.02\text{ cm}^3\text{ g}^{-1}$, and average pore size is 6.1 nm. For the N/S co-doped carbon material, the specific surface area is $886.19\text{ m}^2\text{ g}^{-1}$, the pore volume is $1.6\text{ cm}^3\text{ g}^{-1}$, and the average pore size is 7.2 nm.

3.3. X-ray diffraction of carbon materials

Fig. 5(a) shows small-angle XRD diffraction patterns of the NSCM. The small-angle XRD pattern of SBA-15 shows three well-resolved diffraction peaks associated with six-symmetric (100), (110) and (200) reflections, indicating that SBA-15 has a well-ordered structure.²⁴ The small-angle XRD pattern

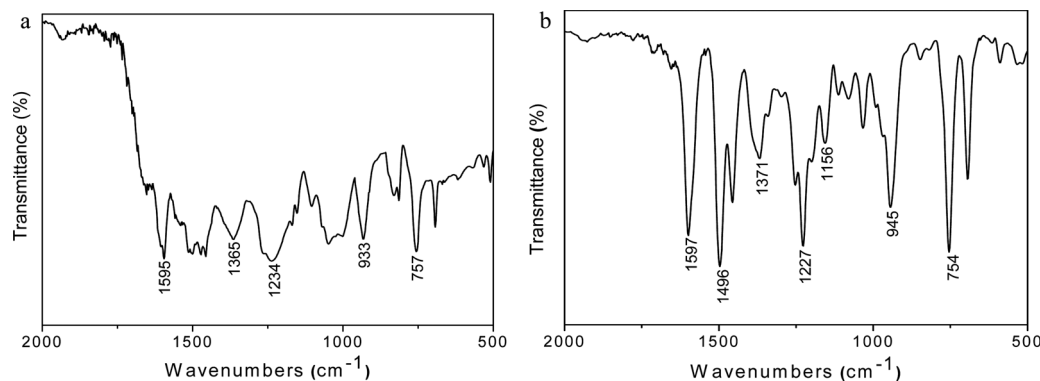


Fig. 3 (a) FTIR spectra of thiourea-type benzoxazine; (b) FTIR spectra of aniline-type benzoxazine.

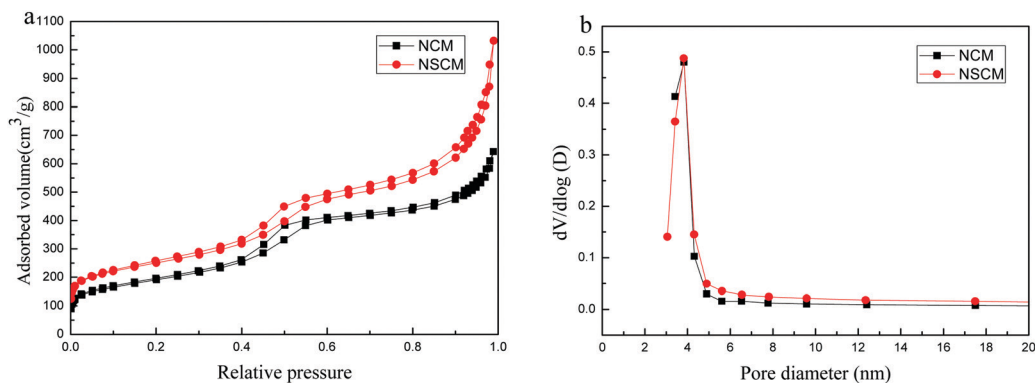


Fig. 4 (a) Nitrogen adsorption-desorption isotherms and (b) pore size distribution curves.

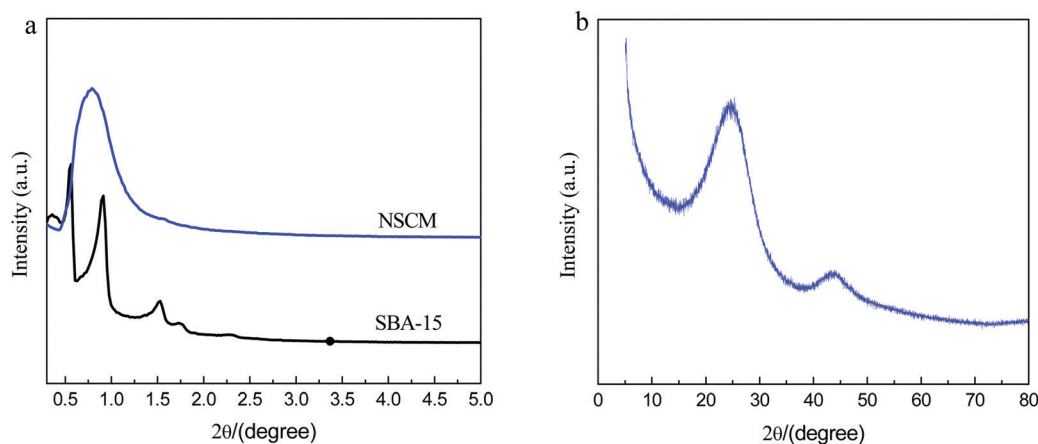


Fig. 5 (a) Small angle XRD pattern of SBA-15 and thiourea-NSCM; (b) wide angle XRD pattern of the thiourea-NSCM.

of the NSCM shows a similar (100) diffraction peak around $2\theta = 0.8^\circ$, which indicates that the order of the pores of the material is reduced compared with SBA-15. The wide-angle XRD pattern of the NSCM is shown in Fig. 5(b), and two diffraction peaks were observed near $2\theta = 25^\circ$ and $2\theta = 44^\circ$, which belong to the diffraction of the (002) and (100) planes of the hexagonal carbon, respectively. The (002) diffraction peak indicates that the lattice spacing of the graphite layer has low crystallinity, and the (100) diffraction peak indicates that the sample has a graphitized amorphous structure.²⁵

3.4. SEM and TEM images of carbon materials

The morphology and microstructure of carbon materials were characterized by SEM and TEM. Fig. 6(a) and (b) are SEM images of NCM and NSCM. It can be seen from the SEM images that both carbon materials exhibit a worm-like structure, which indicates that the carbon material partially replicates the structure and morphology of the template. Fig. 6(c) and (d) are TEM images of NCM and NSCM. As can be seen that both carbon materials are uniform stripe-like and hexagonal arranged structures, which indicates that the carbon materials have an ordered structure. This further proves that the carbon material was successfully copied from the template.²⁶

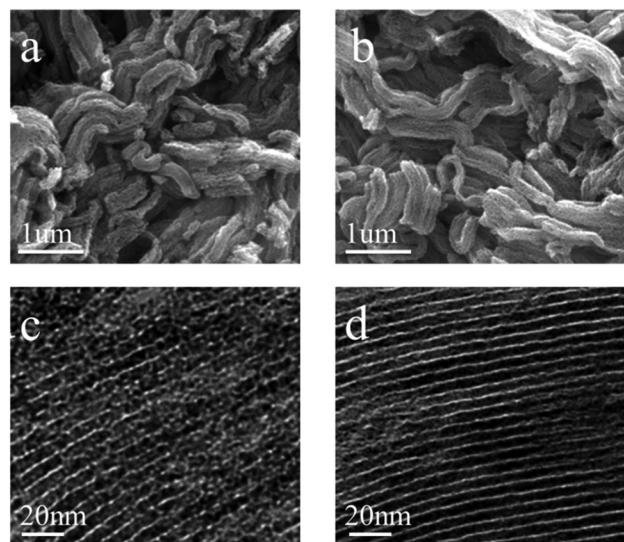


Fig. 6 SEM images of carbon materials and TEM images of carbon materials.

3.5. XPS spectra of carbon materials

Fig. 7 shows the elemental composition of NCM obtained by XPS characterization. There are three absorption peaks in NCM: C

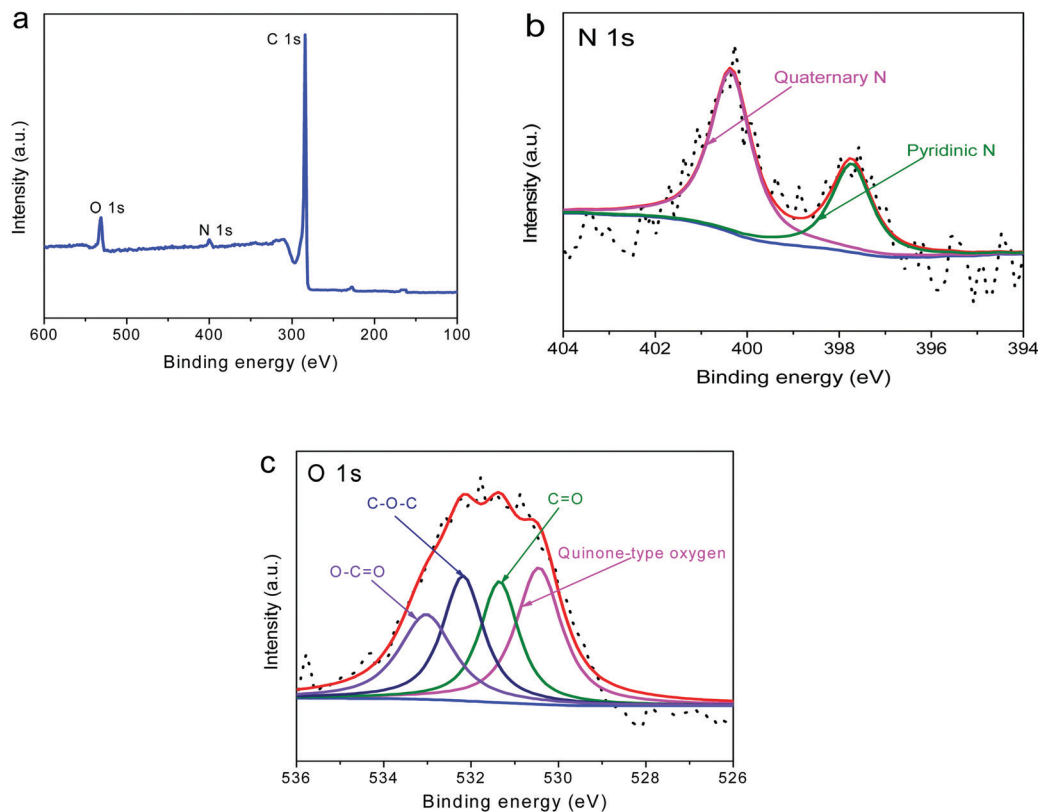


Fig. 7 (a) XPS spectra of NCM; high resolution XPS spectra of N 1s (b) and O 1s (c).

Table 1 Elemental content of the NCM sample

Sample	C (%)	N (%)	O (%)
NCM	89.2	4.95	5.85

(285 eV), N 1s (399.3 eV), O 1s (531.3 eV), and the contents of each element are listed in Table 1. Nitrogen exists in two forms: pyridine-N (397.8 eV) and graphite-N (400.3 eV), and oxygen exists in four forms: quinone oxygen (530.6 eV), C=O (531.3 eV), C-O-C (532.2 eV) and O-C=O (533 eV). The calculated results show that pyridine-N in NCM accounted for 51.3% of the total nitrogen content.

Fig. 8 shows the elemental composition of NSCM obtained by XPS characterization. There are four absorption peaks in NSCM: C 1s (285 eV), N 1s (399.3 eV), S 2p (164.7 eV), O 1s (531.3 eV), and the contents of each element are listed in Table 2. Nitrogen exists in three forms: pyridine-N (397.8 eV), pyrrole-N (399.1 eV), graphite-N (400.3 eV), sulfur exists in two forms: C-S bonds (163.4 eV, 164.6 eV) of thiophene-like sulfur and C-SO_x-C bonds (167.5 eV),²⁷ oxygen exists in two forms: quinone oxygen (530.6 eV) and C-O-C (532.2 eV). We also calculated from Fig. 8(b) that pyridine-N and pyrrole-N together account for 68.2% of the total nitrogen content of NSCM.

Studies^{28,29} on carbon catalysts have shown that the surface defects of carbon materials may be their active sites. The XPS analysis has shown that there are two unsaturated nitrogen,

pyridine-N and pyrrole-N, in the carbon materials. Unsaturated nitrogen will make carbon materials produce surface defects that make carbon materials have certain catalytic activity.³⁰ Compared with NCM, NSCM contains more unsaturated nitrogen, and the addition of sulfur will form a synergistic effect with nitrogen atoms. This effect is beneficial to increase the surface defects of carbon materials.³¹⁻³³ Therefore, the N/S co-doped carbon materials have higher catalytic activity.

3.6. Raman analysis of carbon materials

Fig. 9 shows the results of Raman analysis of carbon materials. The surface defect ratio of carbon materials is expressed by I_D/I_G ,³⁴ and a higher I_D/I_G value suggests the presence of more structural defects. According to the calculation of the analysis results, the surface defect ratio of NCM is 0.95, and the surface defect ratio of NSCM is 1.12. Therefore, NSCM has a higher ratio of surface defects and higher catalytic activity, which also corresponds to XPS analysis. The graphite crystallite sizes of the NCM and NSCM that were calculated using the formula³⁵ are 20.2 nm and 17.2 nm, respectively.

3.7. Catalytic performance

3.7.1. Catalytic performance of NSCM catalysts. In this section, the catalytic performances of NSCM catalysts were systematically studied. The effect of reaction temperature on the progress of the reaction is shown in Fig. 10. At lower temperatures, the reaction proceeds more slowly. With the

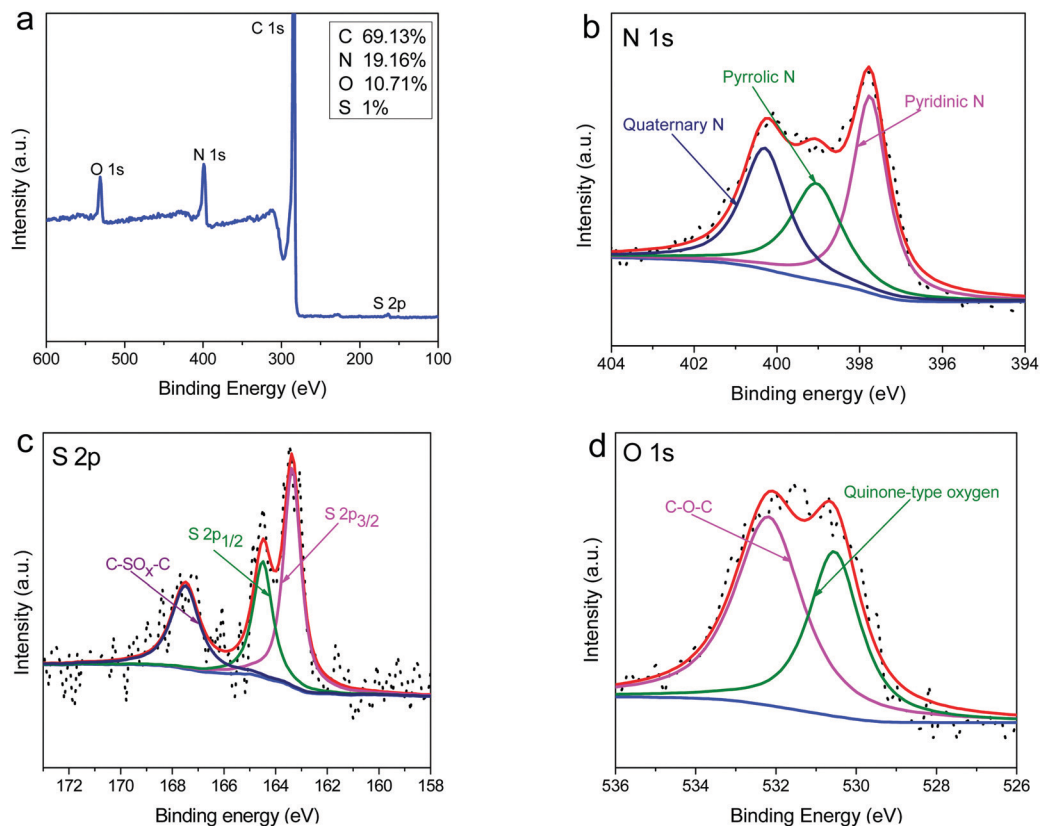


Fig. 8 (a) XPS spectra of NSCM; high resolution XPS spectra of N 1s (b), S 2p (c) and O 1s (d).

Table 2 Elemental content of the NSCM sample

Sample	C (%)	N (%)	O (%)	S (%)
NSCM	69.13	19.16	10.71	1

increase of temperature, the reaction has gradually accelerated, but the selectivity begins to decrease, due to the increase of inside reactions. Considering the effect of temperature on both conversion and selectivity, 85 °C is chosen as the suitable reaction temperature of the N/S co-doped carbon material.

The effect of reaction time on the yield of the target product was studied. As shown in Fig. 11. As the reaction time increases, the conversion rate increases, while the selectivity gradually decreases. This may be due to the increase of supernumerary products which reduces selectivity. Considering the effect of reaction time on both conversion and selectivity, the best reaction time of the N/S co-doped carbon material is 4 h.

The effect of acetic acid has been explored experimentally. Fig. 12 shows the effect of acetic acid on the conversion and selectivity over NSCM catalysts. As the amount of acetic acid increases, the conversion rate increased first and then decreased, while the selectivity increased first, then decreased;

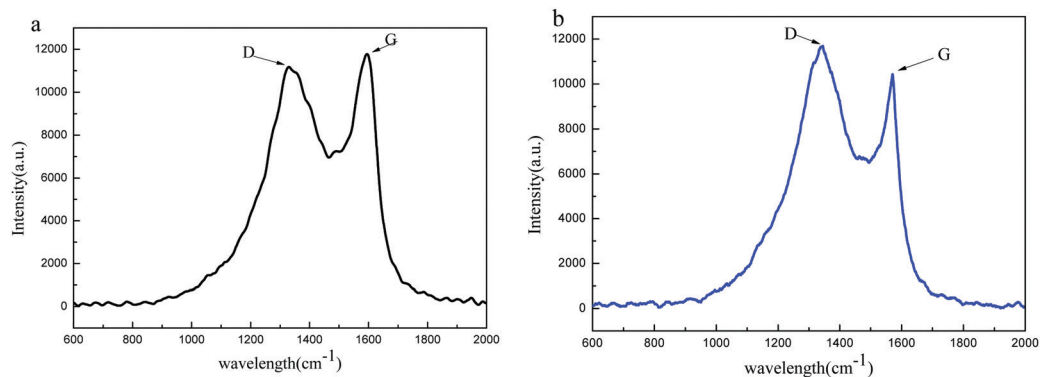


Fig. 9 (a) Raman analysis of NCM, (b) Raman analysis of NSCM.

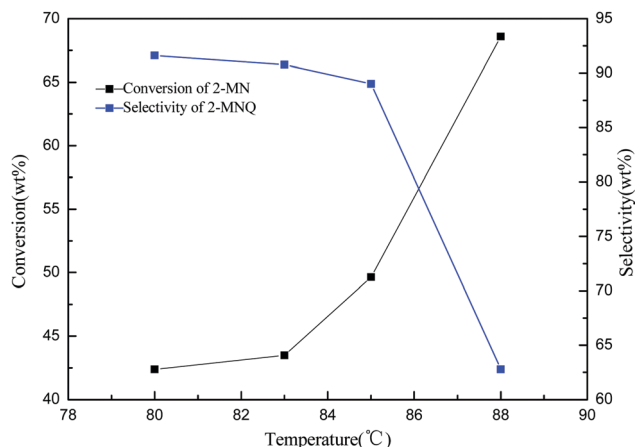


Fig. 10 Effect of reaction temperature on the conversion and selectivity over NSCM. Reaction conditions: reaction time, 4 h; the mass ratio of acetic acid to the raw materials, 26 : 1; the mass ratio of H_2O_2 to the raw materials, 8 : 1; the mass ratio of the raw materials to catalysts, 3 : 1.

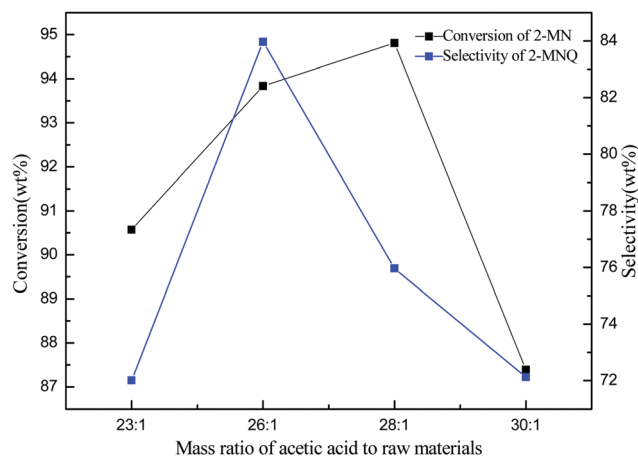


Fig. 12 Effect of acetic acid on the conversion and selectivity over NSCM. Reaction conditions: reaction temperature, 85 °C; reaction time, 4 h; the mass ratio of H_2O_2 to the raw materials, 8 : 1; the mass ratio of the raw materials to catalysts, 3 : 1.

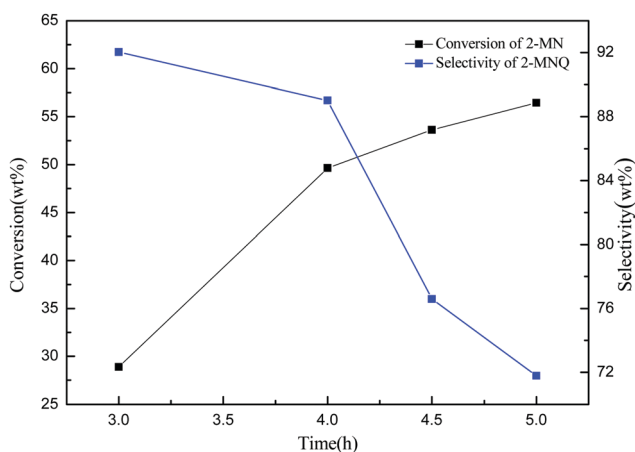


Fig. 11 Effect of reaction time on the conversion and selectivity over NSCM. Reaction conditions: reaction temperature, 85 °C; the mass ratio of acetic acid to the raw materials, 26 : 1; the mass ratio of H_2O_2 to the raw materials, 8 : 1; the mass ratio of the raw materials to catalysts, 3 : 1.

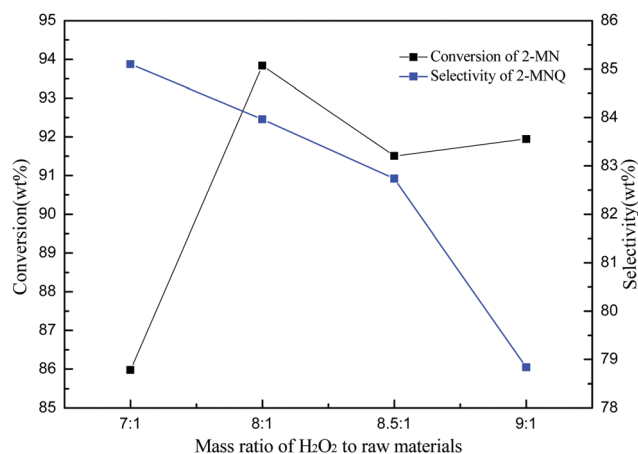


Fig. 13 Effect of H_2O_2 on the conversion and selectivity over NSCM. Reaction conditions: reaction temperature, 85 °C; reaction time, 4 h; the mass ratio of acetic acid to the raw materials, 26 : 1; the mass ratio of the raw materials to catalysts, 3 : 1.

this may be due to the fact that too much acetic acid reduces the concentration of reactants. Considering the yield for the N/S co-doped carbon material, 26 : 1 is selected as the best condition for the mass ratio of acetic acid to raw materials.

Fig. 13 shows the effect of hydrogen peroxide on the catalytic performance of the N/S co-doped carbon material. As the quality of hydrogen peroxide increases, the conversion rate shows the trend of rising first and then falling, while the selectivity has been decreasing. As the quality of hydrogen peroxide further increases, the formation of supernumerary products increases the conversion rate. The optimal mass ratio of H_2O_2 to the raw materials of the N/S co-doped carbon material is 8 : 1.

Finally, the experiment has also explored the effect of the mass ratio of raw materials. The quality of the catalyst is kept constant during the experiments and the mass of the reactants

was changed. Fig. 14 shows the effect of the mass ratio of raw materials on the catalytic activity of the N/S co-doped carbon material. The conversion rate is on the rise, and selectivity begins to decline after reaching its peak. And 3 : 1 is the best mass ratio of raw materials to the catalysts for the N/S co-doped carbon material.

3.7.2. Catalytic performance of the NCM. The catalytic performance of the nitrogen-doped carbon material was investigated through the same scheme as the N/S co-doped carbon material. The best reaction conditions for the nitrogen-doped carbon material obtained from experiments are reaction temperature: 83 °C, reaction time: 5 h, the mass ratio of acetic acid to raw materials: 33 : 1, the mass ratio of H_2O_2 to raw materials: 10 : 1, and the mass ratio of raw materials to catalysts: 4 : 1. The yield of 2-methylnaphthoquinone under optimal reaction conditions is 65.8%. Compared to the two carbon materials, it can

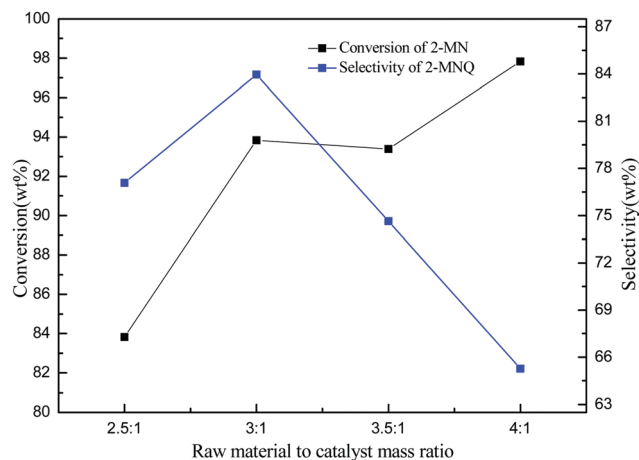


Fig. 14 Effect of the mass ratio on the conversion and selectivity over NSCM. Reaction conditions: reaction temperature, 85 °C; reaction time, 4 h; the mass ratio of acetic acid to the raw materials, 26 : 1; the mass ratio of H₂O₂ to the raw materials, 8 : 1.

Table 3 Results of reusability tests

Reusability test	Conversion/%	Selectivity/%	Yield/%
1	95.51	82.11	78.42
2	94.96	81.93	77.80
3	91.97	84.83	78.02
4	93.13	84.65	78.83
5	92.3	85.75	79.15

be found that the N/S co-doped carbon material has more excellent catalytic activity. The results of catalytic experiments are consistent with those of XPS and Raman characterization of the two materials.

3.7.3. Reusability tests of the NSCM catalyst. For the catalyst, the stability of the catalytic performance is also an important factor. So, the stability of the NSCM catalyst was experimentally investigated. The used catalyst was washed with deionized water and anhydrous ethanol and dried and recycled. The NSCM catalyst was reused five times. The results are shown in Table 3. It can be seen that the NSCM carbon catalyst has good repeatability for this reaction, and the yield after repeated use can be stable at about 78%. After the catalyst was reused five times, we stopped the catalyst repeatability experiment, which means that the catalyst can be used at least five times.

4. Conclusion

The carbon materials prepared from benzoxazine have excellent catalytic performance in 2-methylnaphthalene selective catalytic oxidation reactions. The experimental results show that under the optimal reaction conditions, NSCM and NCM exhibit excellent catalytic activity and the yields of 2-menaquinone are 65.8% and 78.9%, respectively. Upon comparison with literature reports,^{4,5} carbon materials can avoid the problem of metal ion treatment while achieving high conversion rate and high selective catalytic oxidation reaction. The results

have shown that multi-atom doping is more effective for improving the catalytic performance of carbon materials than single-atom doping. The obtained NSCM carbon materials also have good recycling properties and can maintain high catalytic activity after repeated use. We can also know from the study of this paper that compared with some metal catalysts for the 2-methylnaphthalene solid-liquid selective catalytic oxidation reaction, carbon catalysts can obtain higher product yield under relatively mild reaction conditions, and they have relatively steady catalytic performance. We hope that the carbon materials based on benzoxazine should have great potential for advanced applications in the traditional field of chemical heterogeneous catalytic synthesis.

Conflicts of interest

There are no conflicts to declare.

Acknowledgements

This work was supported by the National Natural Science Foundation of China (Grant No. 51703205) and the China Scholarship Council (CSC).

References

- C. Chen, Y. Z. Lin and K. S. Shia, *Bioorg. Med. Chem. Lett.*, 2002, **12**, 2729–2732, DOI: 10.1016/S0960-894X(02)00532-2.
- N. Narender, K. Suresh Kumar Reddy and K. V. V. Krishna Mohna, *J. Porous Mater.*, 2011, **18**, 337–343, DOI: 10.1007/s10934-010-9383-3.
- O. A. Kholdeeva, O. V. Zalomaeva and A. B. Sorokin, *Catal. Today*, 2007, **121**, 58–64, DOI: 10.1016/j.cattod.2006.11.011.
- G. L. Zi, D. M. Chen and B. Li, *Catal. Commun.*, 2014, **49**, 10–14, DOI: 10.1016/j.catcom.2014.01.027.
- S. Uruş and M. Keleş, *Phosphorus Sulfur*, 2010, **7**, 1416–1424, DOI: 10.1080/10426500903061533.
- O. A. Kholdeeva, O. V. Zalomaeva and A. B. Sorokin, *Catal. Today*, 2007, **121**, 58–64, DOI: 10.1016/j.cattod.2006.11.011.
- X. Liu and L. Dai, *Nat. Rev. Mater.*, 2016, 16064, DOI: 10.1038/natrevmats.2016.64.
- Y. Wang and P. Can, *Nanomaterials*, 2019, **9**(3), 439–441, DOI: 10.3390/nano9030439.
- H. Watanabe and S. Asano, *ACS Catal.*, 2015, **5**, 2886–2894, DOI: 10.1021/acscatal.5b00375.
- E. Zeynalov and N. S. Allen, *J. Phys. Chem. Solids*, 2019, **127**, 245–251, DOI: 10.1016/j.jpcs.2018.12.031.
- S. Q. Song, H. G. Yang and R. C. Rao, *et al.*, *Catal. Commun.*, 2010, **11**(8), 783–787, DOI: 10.1016/j.catcom.2010.02.015.
- H. Wang, T. Maiyalagan and X. Wang, *ACS Catal.*, 2012, **2**, 781–794, DOI: 10.1021/cs200652y.
- H. T. Liu, Y. Q. Liu and D. B. Zhu, *J. Mater. Chem.*, 2011, **21**, 3335–3345, DOI: 10.1039/c0jm02922j.
- P. Ayala, R. Arenal and M. Rummeli, *Carbon*, 2010, **48**, 575–586, DOI: 10.1016/j.carbon.2009.10.009.

- 15 D. S. Su, S. Perathoner and G. Centi, *Chem. Rev.*, 2013, **113**, 5782, DOI: 10.1021/cr300367d.
- 16 Y. Wang, J. S. Zhang and X. C. Wang, *Angew. Chem., Int. Ed.*, 2010, **49**, 3356–3359, DOI: 10.1002/anie.201000120.
- 17 H. Yu, F. Peng and J. Tan, *Angew. Chem., Int. Ed.*, 2011, **123**, 4064–4068, DOI: 10.1002/anie.201007932.
- 18 J. L. Long, X. Q. Xie and J. Xu, *ACS Catal.*, 2012, **2**, 622–631, DOI: 10.1021/cs3000396.
- 19 Y. J. Gao, G. Hu and J. Zhong, *Angew. Chem., Int. Ed.*, 2013, **52**, 2109–2113, DOI: 10.1002/anie.201207918.
- 20 S. Van Dommele, K. P. De Jong and J. H. Bitter, *Chem. Commun.*, 2006, 4859–4861, DOI: 10.1039/b610208e.
- 21 A. Villa, J. P. Tessonnier and O. Majoult, *ChemSusChem*, 2012, **3**, 241–245, DOI: 10.1002/cssc.200900181.
- 22 X. L. Gao, X. B. Sun and L. Xu, *J. Mater. Res.*, 2019, **34**(7), 1219–1228, DOI: 10.1557/jmr.2019.92.
- 23 X. M. Fan, C. Yu and J. Yang, *Carbon*, 2014, **70**, 130–141, DOI: 10.1016/j.carbon.2013.12.081.
- 24 Y. R. Liu, *J. Porous Mater.*, 2014, **21**(6), 1009–1014, DOI: 10.1007/s10934-014-9850-3.
- 25 S. M. Liu, Y. J. Cai and X. Zhao, *J. Power Sources*, 2017, **360**, 373–382, DOI: 10.1016/j.jpowsour.2017.06.029.
- 26 N. N. Liu, L. W. Yin and C. X. Wang, *Carbon*, 2010, **48**, 3579–3591, DOI: 10.1016/j.carbon.2010.06.001.
- 27 W. Li, M. Zhou and H. M. Li, *Energy Environ. Sci.*, 2015, **8**(10), 2916–2921, DOI: 10.1039/C5EE01985K.
- 28 J. Zhang, X. Liu and R. Blume, *et al.*, *Science*, 2008, **322**(5898), 73–77, DOI: 10.1126/science.1161916.
- 29 J. Zhang, D. S. Su and R. Blume, *et al.*, *Angew. Chem., Int. Ed.*, 2010, **49**(46), 8640–8644, DOI: 10.1002/anie.201002869.
- 30 D. Wei, Y. Liu and Y. Wang, *et al.*, *Nano Lett.*, 2009, **9**(5), 1752–1758, DOI: 10.1021/nl803279t.
- 31 A. Lin and Z. Y. Zhang, *Chem. Eng. J.*, 2017, **313**, 1320–1327, DOI: 10.1016/j.cej.2016.11.025.
- 32 W. J. Tian, H. Y. Zhang and X. G. Duan, *et al.*, *ACS Appl. Mater. Interfaces*, 2016, **8**, 7184–7193, DOI: 10.1021/acsami.6b01748.
- 33 H. Liu, P. Sun and M. Feng, *Appl. Catal., B*, 2016, **187**, 1–10, DOI: 10.1016/j.apcatb.2016.01.036.
- 34 M. Knauer, M. E. Schuster and D. Su, *et al.*, *J. Phys. Chem. A*, 2009, **113**, 13871–13880, DOI: 10.1021/jp905639d.
- 35 L. G. Cancado, K. Takai and T. Enoki, *Appl. Phys. Lett.*, 2006, **88**, 163106, DOI: 10.1063/1.2196057.